EPJ manuscript No.
(will be inserted by the editor)

Fracture of a biopolymer gel as a viscoplastic disentanglement process

Tristan Baumberger, Christiane Caroli & David Martina

INSP, Université Pierre et Marie Curie-Paris 6, Université Denis Diderot-Paris 7, CNRS, UMR 7588 Campus Boucicaut, 140 rue de Lourmel, 75015 Paris, France.

February 6, 2008

Abstract. We present an extensive experimental study of mode-I, steady, slow crack dynamics in gelatin gels. Taking advantage of the sensitivity of the elastic stiffness to gel composition and history we confirm and extend the model for fracture of physical hydrogels which we proposed in a previous paper (Nature Materials, doi:10.1038/nmat1666 (2006)), which attributes decohesion to the viscoplastic pull-out of the network-constituting chains. So, we propose that, in contrast with chemically cross-linked ones, reversible gels fracture without chain scission.

PACS. 62.20.-Mk Mechanical properties of solids – 83.80.Km Physical gels and microgels – 83.60.La Viscoplasticity, yield stress

1 Introduction

Hydrogels are a family of materials constituted of a sparse random polymer network swollen by a (most often aqueous) solvent. They can be classified into two subgroups.

– *Chemical gels*, such as polyacrylamid ones, in which the cross-links (hereafter abbreviated as CL) between the polymer chains are made of single covalent molecular bridges. Their gelation process is irreversible.

– *Physical gels* in which cross-linking is due to hydrogen or ionic bonds, much weaker than covalent ones. In most of them the network is constituted of biopolymers [1], e.g. proteins (gelatin) or polysaccharides (agar, alginates). Due to stabilizing steric interactions, these CL may involve many monomeric units (residues), extending over lengths of several nanometers. Such is the case for gelatin gels. Gelatin results from the denaturation of collagen, whose native triple helix structure is locally reconstituted in the CL segments, interconnected in the gel by flexi-

Correspondence to: tristan@insp.jussieu.fr

ble segments of single protein chains. Due to the weak strength of their CL bonds, physical gels are thermoreversible. For example, gelatin networks "melt" close above room temperature. This behavior leads to the well studied slow ageing (strengthening) of their elastic modulus [2], and to their noticeable creep under moderate stresses [3].

Biopolymer based physical gels have been attracting increasing interest motivated by their wide use in the food industry [4] and to promising biomedical developments in fields such as drug delivery and tissue engineering [5]. All these implementations call for the control of their mechanical properties – namely elastic stiffness and fracture toughness, independent tuning of which would be highly desirable.

While elastic responses of gels have been extensively studied, both in the small [1] [2] and large deformation regimes [6] [7], fracture studies have been up to now essentially concerned with crack nucleation [8] and ultimate strength measurements [6] [7]. However, trying to elucidate the nature of the dissipative processes at play in fracture, which are responsible for the rate dependence of their strength, naturally leads to investigating the propagation of cracks independently from their nucleation. Tanaka *et al* [9] have performed such a study on chemical polyacrylamid/water gels. By changing the concentration of cross-linking agent at fixed polymer content, they found that, in this material, stiffness and toughness are negatively correlated : as is the case for rubbers, the stiffer the gel is, the smaller its fracture energy. More recently, Mooney *et al* [10] have been able to compare the fracture behavior of chemically and physically cross-linked alginate gels. They showed that the stiffness/toughness correlation, while agreeing with Tanaka's result for covalent CL, is inverted for ionic ones. In this latter case "the stiffer the tougher".

We report here the results of an extensive study of steady, strongly subsonic, mode-I (opening) crack propagation in gelatin gels. This choice was made for several reasons. First, due to their massive industrial use, their elastic properties and molecular structures have been thoroughly studied. On the other hand, they can be easily cast into the large homogeneous samples required for fracture experiments. Morevover, solvent viscosity can be tuned by using glycerol/water mixtures.

We have studied the dependence of the fracture energy $\mathcal{G}$ on the crack velocity V for gels differing by their gelatin concentration c, glycerol content ϕ, and thermal history, each of which is known to affect their elastic properties. Experimental methods are described in Section 2. We present in Section 3. the behavior of $\mathcal{G}(V)$ for 3 different series of samples :

A — Common c and history, variable ϕ (hence solvent viscosity η_s).

B — Fixed c and ϕ, different histories.

C — Common ϕ and history, variable c.

We discuss and interpret these results in Section 4. As already reported in [11], the analysis of solvent effects (series A) leads us to propose that, in contradistinction

with chemical hydrogels, physical ones do not fracture by chain scission, but by viscous pull-out of whole gelatin chains from the network via plastic yielding of the CL. This interpretation properly accounts for the quasi-linear dependence of $\mathcal{G}$ on $\eta_s V$ as well as for the orders of magnitude of its slope $\Gamma = d\mathcal{G}/d(\eta_s V)$ and of its quasi-static limit $\mathcal{G}_0$. We then turn toward the variations of Γ with the small strain shear modulus μ^*. We find that our fracture scenario, when combined with the model proposed by Joly-Duhamel *et al* [12] for gelatin network structure and elasticity, is compatible with the results from series B. One step further, the analysis of the effect of gelatin concentration variations (series C) leads us to invoke a concentation-dependent effective viscosity affecting the viscous drag on chains pulled out of the gel matrix.

2 Experimental methods

2.1 Sample preparation

The gels are prepared by dissolving gelatin powder (type A from porcine skin, 300 Bloom, Sigma) in mixtures containing a weight fraction ϕ of glycerol in deionized water, under continuous stirring for 30 min at 90°C. This temperature, higher than commonly used ones ($\sim$ 50 - 60°C) has been chosen, following Ferry [13], so as to obtain homogeneous pre-gel solutions even at the highest ϕ (60 %). A control experiment carried out with a (pure water)/gelatin sample prepared at 60° C resulted in differences of low strain moduli and Γ values of, respectively, 1 % and 7 %, compatible with scatters between 90°C samples. So, we concluded that our preparation method does not, as might have been feared, induce significant gelatin hydrolysis.

The pre-gel solution is poured into a mould consisting of a rectangular metal frame and two plates covered with Mylar films. On the longest sides of the frame, the curly part of an adhesive Velcro tape improves the gel plate grip. Unless otherwise specified (see Section 3.2, series B results), the thermal history is fixed as follows. The mould is set at 2±0.5°C for 15 h, then clamped to the mechanical testing set-up and left at room temperature (19±1 °C) for 1 h. This waiting time ensures that variations of elastic moduli over the duration of the subsequent run can be safely neglected [2]. The removable pieces of the mould are then taken off, leaving the $300\times30\times10$ mm^3 gel plate fixed to its grips. The Mylar films are left in position to prevent solvent evaporation. They are peeled off just before the experiment.

2.2 Gel characterization

For each fracture experiment we prepare simultaneously two nominally identical samples, one of which is used to determine the elastic characteristics. For this purpose, with the help of the mechanical set up described below, we measure the the force-elongation response $F(\lambda)$ of the plate (see Fig. 1), up to stretching ratios $\lambda = 1.5$, at the loading rate $\dot{\lambda} = 1.7\ 10^{-2}$ sec^{-1}.

From these data, we extract an effective small strain shear modulus μ^*. In hydrogels, while shear stresses are sustained by the network, pressure is essentially borne by

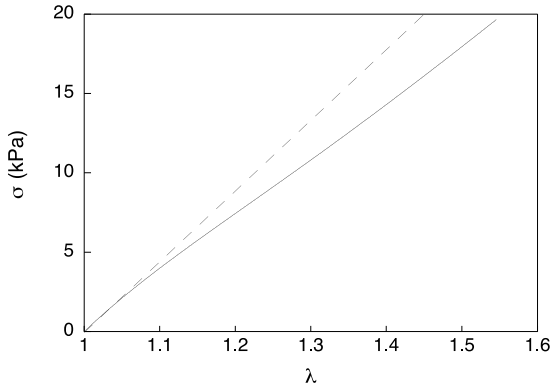

Fig. 1. Nominal stress $\sigma = F/(e_0 L_0)$ versus stretching ratio for a $c = 10$ wt%, $\phi = 0$ wt% sample plate. The dashed line is the extrapolation of the small strain linear response. Its slope is four times the effective shear modulus $\mu^* = 11$ kPa (see text).

the solvent. Hence, since shear moduli are typically in the 1 - 10 kPa range, the gels can be considered incompressible (Poisson ratio $\nu = 1/2$), as long as no solvent draining occurs [14]. So, the sound velocity relevant to define the subsonic regime is the transverse one $c_s = \sqrt{\mu/\rho}$, with ρ the gel mass density. For our systems, typically $c_s \sim 1$ m.sec^{-1}. Neglecting finite size effects, we assume plane stress uniform deformation for our plates of undeformed length $L_0 = 300$ mm, width $h_0 = 30$ mm, thickness $e_0 = 10$ mm. In the linear regime, this assumption leads us to define a (necessarily somewhat overestimated) effective modulus as $\mu^* = \frac{1}{4}\left(\frac{d\sigma}{d\lambda}\right)_{\lambda=0}$, with $\sigma = F/(e_0 L_0)$ the nominal stress, $\lambda = h/h_0$ the stretching ratio, h the stretched width.

One step further, and under the conservative assumption that small strain elasticity is basically of entropic origin, we extract a length scale characteristic of the network as $\xi = (k_B T/\mu^*)^{1/3}$, which lies in the 10 nm range. This order of magnitude agrees with the one which can be evaluated from measurements of the collective diffusion coefficient D_{coll} which characterizes the solvent/network relative motion [14] [15].

For gelatin/water samples [16], $D_{coll} \sim 10^{-11}$ m^2/sec, so that a typical time scale for draining over $\sim$ 1cm is on the order of 10^7 sec, which means that macroscopic stress-induced draining is totally negligible here.

As can be seen on Figure 1, beyond λ values on the order of 1.1, the force response markedly departs from its small strain linear behavior. In order to calculate the mechanical energy released per unit area of crack extension, conventionally termed energy release "rate" $\mathcal{G}$, we need to compute the elastic energy $\mathcal{F}(\lambda)$ stored in the stretched plate. For this purpose we integrate numerically the measured response curve.

2.3 Fracture experiments

The mechanical set-up is sketched on Figure 2. One of the grips holding the gel plate is clamped to the rigid external frame. The other one is attached to one end of a double cantilever spring of stiffness $K = 43.1 \times 10^3$ N.m^{-1}. The other end of the spring can be displaced by a linear translation stage, with a 0.1μm resolution. The deflection of the spring is measured by four strain gauges glued to the spring leaves, with a resolution of $5.10^{-2}\mu$m.

In most runs, the sample stiffness is much smaller than the spring one, and fracture occurs in the so-called fixed

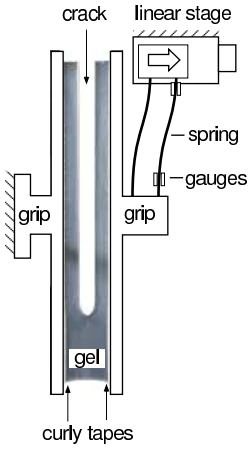

Fig. 2. Schematic representation of the mechanical setup, drawn around a genuine photograph of a gel plate (c = 10 wt%, ϕ = 0 wt%), stretched to $\lambda = 1.5$. Note that the crack propagates straight along the mid-plane. The light blue hue of the gel (color on line) results from Rayleigh scattering by small scale gel network randomness.

grips configuration. The stretching ratio λ is computed in all cases by subtracting the spring deflection amplitude from the stage displacement.

Before stretching, a knife cut of length 20 mm is made at mid-width at the upper free gel edge. In a first set of experiments the grips are pulled apart for 1 sec up to the desired amount Δh. The resulting crack advance is monitored by a camera with a 631 × 491 pix^2 CCD device operating at a typical rate of 15 sec^{-1}. The crack tip position is measured with 0.5 mm resolution. The crack velocity V is obtained from a sliding linear regression over 5 successive position data.

Away from the sample edges, in this configuration, cracks run at constant velocity [1]. As expected, the free edges affect crack propagation up to a distance comparable with the plate width. Further data processing has been systematically restricted to the central region, extending over $\sim$ 200 mm. In this region, we can legitimately compute the energy release rate as [17] $\mathcal{G} = \mathcal{F}/(e_0 L_0)$.

Such experiments result in one run producing one single $\mathcal{G} - V$ data point, hence are very time consuming. So, in a second set of experiments, the stretching ratio was increased at the constant rate $\dot{\lambda} = 1.7\ 10^{-2}$ sec^{-1}. This results in a slowly accelerating crack. We have validated the corresponding $\mathcal{G}(V)$ data by comparison with steady state ones on an overlapping velocity range (see Fig. 3). The crack dynamics in this latter type of experiments can therefore be termed "quasi-stationary".

3 Experimental results

3.1 Solvent effects

We summarize here the results, already reported in reference [11], corresponding to series A, namely gels prepared as described above, with gelatin concentration $c = 5$ wt%, glycerol content ranging from 0 to 60 wt%, i.e. solvent viscosity η_s from 1 to 11 times that of pure water.

[1] This is true for not too small velocities, where bulk creep during a run is negligible. For slow cracks, with velocities below a few hundred μm.sec^{-1}, creep results in a measurable velocity drift. We only retain data out of this range.

As shown on Figure 3, for all samples $\mathcal{G}$ increases quasi-linearly with V in the explored range and, within experimental accuracy, the various curves extrapolate to a common, ϕ-independent value $\mathcal{G}(V \to 0) = \mathcal{G}_0$ which yields an evaluated quasi-static toughness. This cannot be accessed directly. Indeed, the above mentioned importance of creep in our gels leads to the well-known problems met when trying to define static threshold in weak solids (such as colloidal gels, pastes,...). For this series, we find $\mathcal{G}_0 \simeq 2.5$ J m^{-2}, a value about 20 times smaller than a gel-air surface energy.

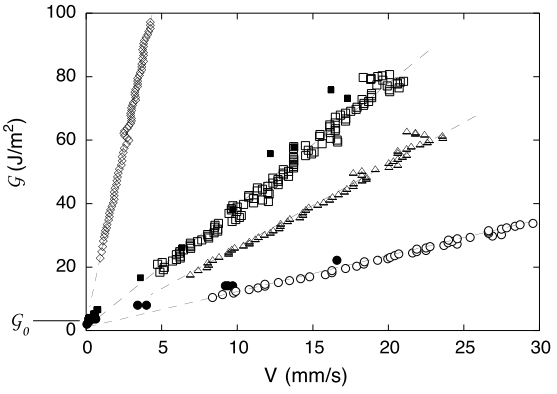

Fig. 3. Fracture energy release rate for gels with the same gelatin concentration ($c = 5$ wt%) and various glycerol contents (series A): $\phi = 0$ wt% (circles), 20 wt% (triangles), 30 wt% (squares), 60 wt% (diamonds). Filled symbols correspond to stationary cracks, open symbols to cracks accelerated in response to a steady increase of λ. $\mathcal{G}_0 = 2.5 \pm 0.5$ J.m^{-2} is the common linearly extrapolated toughness. From ref. [11]. (reprinted from Nature Materials).

Moreover, the slope $d\mathcal{G}/dV$ strongly increases with ϕ, which suggests that $\eta_s V$ might be the relevant variable.

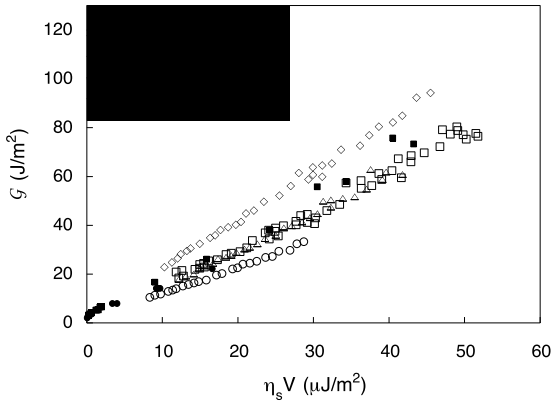

Fig. 4. Same data as Fig. 3 replotted versus $\eta_s V$, with η_s the viscosity of the glycerol/water solvent. From ref. [11]. (reprinted from Nature Materials).

Indeed, the corresponding plot (Fig. 4) captures most of this variation. We therefore write

$$\mathcal{G} = \mathcal{G}_0 + \Gamma\, \eta_s V \qquad (1)$$

The dimensionless slope Γ is found to be a huge number, of order 10^6. In Section 4 below, we will relate the variations of Γ with those of the elastic modulus μ^*. Figure 5 shows that, within series A, Γ increases with μ^*.

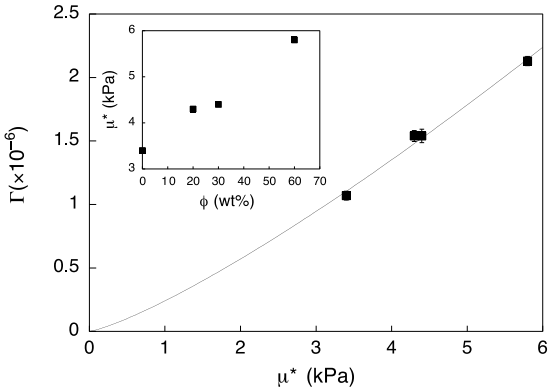

Fig. 5. Rate sensitivity $\Gamma = d\mathcal{G}/d(\eta_s V)$ vs. μ^* for the samples of series A. The line is the best power law fit $\Gamma \sim \mu^{*1.2}$. Insert shows that increasing the glycerol content stiffens the gel.

The quasi-scaling of $\mathcal{G}$ with $\eta_s V$ points toward the critical role of polymer-solvent relative motion in the fracture process. In order to shed further light on this point, we have also performed, with the same gels, experiments in which a small drop of solvent is introduced into the already moving crack opening. For such wetted cracks, as shown on Figure 6, $\mathcal{G}(V)$ is simply shifted downward by a constant amount $-\Delta\mathcal{G}_0$, its slope remaining unaffected. The energy cost $\Delta\mathcal{G}_0 \sim 2$ J m^{-2}, a substantial fraction of $\mathcal{G}_0$. It clearly signals that, in the non-wetted tip case, fracture involves exposing gelatin chains to air. Such local solvent draining into the gel bulk is likely to result from the impossibility for our not very thin incompressible plates to accommodate the high strain gradients which develop close to the tip without being the seat of high negative fluid pressures.

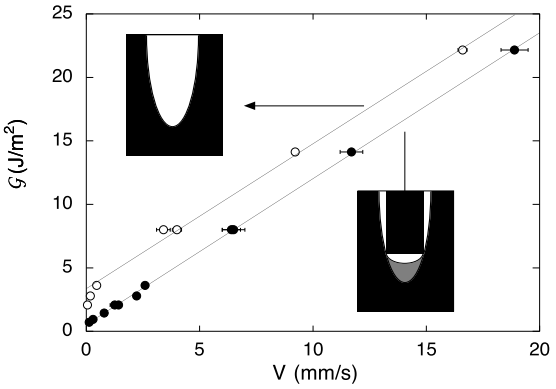

Fig. 6. $\mathcal{G}(V)$ curves for a 5 wt% gelatin gel in pure water : "dry" cracks opening in ambient air (upper data) and "wet" cracks with a drop of pure water soaking the tip. At $\mathcal{G}$ too low for dry cracks to propagate, wet ones can still run. Linear fits are shown. The wet data appear merely translated towards lower energies. The extrapolated fracture energy for wet tips is $\mathcal{G}_0^{wet} = 0.6 \pm 0.15$ J.m^{-2}. From ref. [11]. (reprinted from Nature Materials).

3.2 History-controlled stiffness effects

In a static situation, the solvent would get sucked from the bulk into the tip region, leading to gradual smearing out of the fluid pressure gradient. However, in the steadily moving case, the space range of this collective diffusion process is limited to $\sim D_{coll}/V$ [18] [19]. For tip velocities above ~ 1 mm sec^{-1}, this length is smaller than the mesh size ξ, and the process is inefficient. For much slower cracks, it would lead to a long transient towards a lower apparent $\mathcal{G}_0$. Trying to disentangle this from creep effects, which also become relevant for slow cracks, will demand a detailed characterization of creep which is out of the scope of this paper.

The results for series A above suggest a positive correlation between the slope Γ and the small strain modulus μ^*. In a second set of experiments, we have tuned μ^* at two different gel compositions, namely $\phi = 0$, $c = 10$ and 15 wt%. This was realized by taking advantage of the rather strong dependence of μ^* on the temperature maintained during gelation, as well as on the duration of the gelation phase itself [2] [12] (always chosen large enough for μ^* variations to remain negligible during the run). This enabled us to induce μ^* values differing by at most a factor of 2. The data are shown on Figure 7. It is seen that, for each c-value, again, the stiffer the gel, the tougher. Note, however, that Γ is not a function of μ^* only, but also of

composition - a point which will be discussed in detail in Section 4.

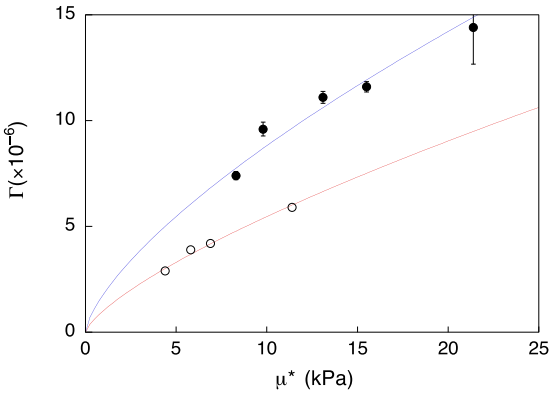

Fig. 7. Γ vs. μ^* for gels from series B ($\phi = 0$, various thermal histories). $c = 15$ wt% (full dots); $c = 10$ wt% (open circles). The curves are guide for the eye.

3.3 Gelatin concentration effects

We have investigated this last point directly by working with a third set of samples (series C) with the common history described in section 2, the same solvent (pure water) and different values of c. As already amply documented [1] [12], μ^* increases with c (Fig.8). A power law fit yields $\mu^* \sim c^{1.64\pm0.2}$. This exponent, somewhat lower than usual values ($\lesssim 2$), is close to that measured by Bot *et al* [6]. Figure 8 also shows the $\Gamma(\mu^*)$ data. Once more, $d\Gamma/d\mu^* > 0$.

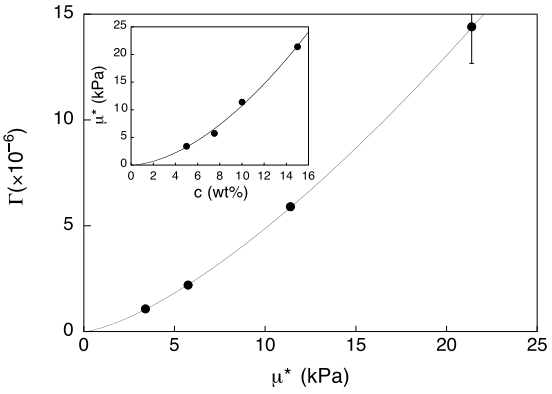

Fig. 8. Γ vs. μ^* for gels from series C ($\phi = 0$, various gelatin concentrations). Insert shows μ^* vs. c. The full lines are the power law fits (see text).

4 Discussion and interpretation

4.1 A viscoplastic model of gelatin fracture

At first glance, as far as fracture is concerned, our gels share two salient features with another class of soft elastic materials, namely rubbers [20] [21]. In both cases :

(1) the toughness $\mathcal{G}_0$ is at least one order of magnitude larger than the energy of the surfaces created by the crack advance.

(2) $\mathcal{G}$ increases rapidly with V in the strongly subsonic regime.

Hence a first question : are the physical mechanisms now well established to be responsible for these two features in the case of rubbers also at work for our physical gels?

The basic theory of rubber toughness was formulated by Lake and Thomas [20]. Fracture occurs via chain scission : the polymer segments, of areal density Σ, crossing the fracture plane are stretched taut until they store an

elastic energy per monomer on the order of the covalent monomer-monomer bond one, $U_{chain} \sim$ a few eV. At this stage, each of them sustains a force $f_{chain} \sim U_{chain}/a$, with a a monomer size. A bond-breaking event thus corresponds to dissipating all of the elastic energy that was stored in the whole segment (n monomers) joining two cross-links, $\sim nU_{chain}$. So, $\mathcal{G}_0^{(rub)} \sim nU_{chain}\Sigma$, an expression which explains the order of magnitude of $\mathcal{G}_0$ as well as its decrease when stiffness increases (the stiffer a rubber is, the less tough).

The V-dependent fracture energy of rubbers is of the form [22] [23]

$$\mathcal{G}^{(rub)}(V) = \mathcal{G}_0^{(rub)}[1 + \Phi(a_T V)] \tag{2}$$

where a_T is a temperature dependent WLF-like factor. This velocity dependence has been shown to result from bulk viscoelastic dissipation [24] [25]. Due to the stress gradients ahead of the moving crack, which extend far beyond the "active tip zone" where decohesion takes place, the material deforms at a strain rate which sweeps its whole relaxation spectrum, hence the WLF scaling factor. That $\mathcal{G}_0^{(rub)}$ factors out in expression (2) results from two facts [26] : (i) linear elasticity preserves the universal $r^{-1/2}$ stress concentration field (ii) the so-called small scale yielding assumption holds, namely the size of the active zone is negligible as compared with that of the viscous dissipating one.

We will now argue that none of these mechanisms is relevant in our case.

On the one hand, we claim that, in physical gels, fracture cannot process via chain scission. Indeed, the force f_{chain} defined above is more than one order of magnitude larger than that, $f^* \simeq U_{CL}/a$, which can be sustained by the H-bond stabilized cross-links. Clearly, when the stored elastic energy reaches $\sim U_{CL}$ per monomer, CL bonds yield, by either unzipping [27] [28] or frictional sliding [29]. This leads us to postulate that, in the highly stressed active tip zone, the chains which cross the crack plane creep until they are fully pulled out of the gel matrix. The threshold stress at the onset of CL yielding is $\sigma^* = f^*\Sigma$, with Σ the areal density of crossing chains. As a rough estimate for this density we take $\Sigma \sim 1/\xi^2$, with

$$\xi = \left(\frac{k_B T}{\mu^*}\right)^{1/3} \tag{3}$$

the above-defined estimate of the mesh size of the polymer network. Then, with $a \sim 0.3$nm, $U_{CL} \sim 0.1$eV, $\xi \sim 10$nm, we obtain $\sigma^* \sim 500$kPa.

Note that, contrary to standard conditions met with hard materials, here $\sigma^*/\mu^* \gg 1$ ($\sim 10^2$), which makes the issue of elastic blunting raised by Hui *et al* [30] certainly relevant to gel fracture.

When solvent can be pumped from a wetting drop (see Section 3.1), the plastic zone deforms under this constant stress until the opening δ_c at the tip reaches the length of the chain - i.e. its full contour length l, since at this stress level it is pulled taut. This is precisely the well-know Dugdale model of fracture [31], which yields, for the quasi-static fracture energy of wet cracks :

$$\mathcal{G}_0^{wet} = \sigma^* l \tag{4}$$

From series A resuts, we estimate $\mathcal{G}_0^{wet} \approx 0.6 \pm 0.15$ J m^{-2}. This, together with expression (4), enables us to get an estimated chain contour length $l \sim 1.2\mu$m. With an average mass $M_{res} = 80$ g/mole for each of the l/a residues, this means a reasonable 300 kg order of magnitude estimate for the gelatin molar weight.

In this picture, we interpret the shift $\Delta\mathcal{G}_0 = \mathcal{G}_0 - \mathcal{G}_0^{wet}$ as an energy cost associated with chain extraction out of the solvent. This yields for the solvation energy per chain $\Delta\mathcal{G}_0\xi^2 \sim 1000$ eV, i.e. $\sim 10 k_B T$ per residue.

Let us now turn to the V-dependence of $\mathcal{G}$. The tip wetting experiments (see Figure 6) directly show that $\mathcal{G}_0$ and the slope Γ are independent : wetting shifts $\mathcal{G}_0$ while leaving Γ unaffected. We consider that this empirical argument by itself rules out bulk viscoelasticity as the controlling mechanism. This appears all the more reasonable that rheological studies [2] [13] show that viscous dissipation in hydrogels (loss angles typically $\lesssim 0.1$) is much smaller than that in rubbers.

We are therefore led to extend our fracture model to finite velocities. A finite V means a finite average pull-out velocity $\dot{\delta} = \alpha V$, where α is a geometrical factor characteristic of the shape of the Dugdale zone. Pull-out implies motion of the network relative to the solvent, hence a viscous contribution to the viscoplastic tip stress :

$$\sigma_{tip} = \sigma^* + \sigma_{vis}(V) \tag{5}$$

Solvent/network relative motion is diffusive [14], which implies that fluid pressure gradients obey a Darcy law with an effective porosity $\kappa = \eta_s D_{coll}/\mu$, which can be expected on dimensional grounds to scale as ξ^2. Baumberger *et al* [16] have shown that, for gelatin gels such as used in this work, $\kappa/\xi^2 \simeq 6.10^{-2}$. We thus estimate σ_{vis} as resulting from the build up of the Darcy pressure over a length $\sim l$, i.e.

$$\sigma_{vis} \sim l\,(\nabla p)_{Darcy} \sim \frac{l\eta_s\dot{\delta}}{\kappa} \tag{6}$$

and

$$\begin{aligned}\mathcal{G}(V) &\approx \mathcal{G}_0 + l\sigma_{vis} \\ &= \mathcal{G}_0 + \alpha\frac{l^2}{\kappa}\eta_s V\end{aligned} \tag{7}$$

which exhibits the observed linear variation with $\eta_s V$ and predicts that the slope

$$\Gamma = \alpha\frac{l^2}{\kappa} \tag{8}$$

We found (Section 3.1) that Γ is of order 10^6. With l as evaluated above and $\xi \sim 10$ nm, we get from expression (8) $\Gamma \approx 2.10^5\alpha$, which suggests that α should be of order 1 at least. In the Dugdale model, one gets :

$$\alpha = \frac{\delta_c}{d_{act}} \approx \frac{\sigma^*}{\mu} \tag{9}$$

For hard solids, σ^* is the plastic yield stress σ_Y, always $\ll \mu$. We pointed out that, for physical gels, on the contrary, $\sigma^*/\mu \gg 1$. The Dugdale analysis can certainly not be directly used here, due to the very large deformation levels involved, hence to problems such as elastic blunting, strain-hardening and strain induced helix-coil transitions [32]. We were able, with the help of a hetero-wetting experiment (pure water wetting a crack tip in a glycerolled gel) reported in [11], to obtain a direct evaluation of the size of the active zone. It yielded $d_{act} \sim 100$ nm, from which we expect that $\alpha = l/d_{act} \sim 10$.

We should point out that our model for tip dissipation (Eq. (5)) is formally identical to that put forward by Raphael and de Gennes [33] in the context of rubber-rubber adhesion with connector molecules. But in the gel case, where viscous dissipation is controlled by solvent-network friction, the very large compliances involved cast doubt on the legitimity of mathematical treatments based upon small opening and linear elasticity approximations [33] [34]. However, the possibility of accessing d_{act}, and thus the fracture parameter α experimentally, together with the absence of substantial bulk viscoelastic dissipation enable us to conclude that our fracture model is consistent with experiments as far as :

– it accounts for the linear dependence of $\mathcal{G}$ on $\eta_s V$.

– it yields reasonable orders of magnitude for the quasi-static toughness and the slope Γ.

4.2 Relationship between fracture and elastic properties

For further confirmation we now need to test the predictions of the model against the measured variations of Γ with small strain elastic modulus μ^*.

Let us first consider the results of series B, involving gels with the same composition but various thermal histories. According to equation (8) we predict that, for each such set of samples, Γ should scale as κ^{-1}, i.e. as :

$$\Gamma \approx \mu^{2/3} \qquad (10)$$

As seen on Figure 9, the agreement with experimental data is quite satisfactory, bringing good support to the model.

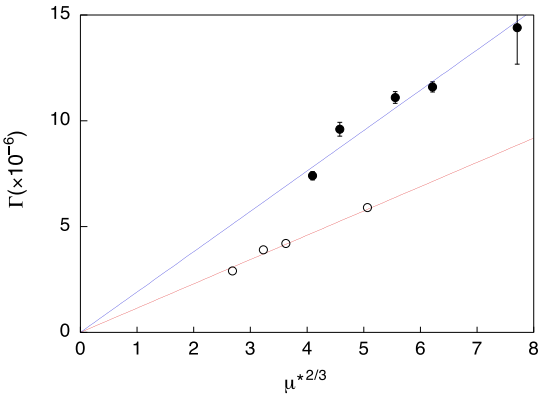

Fig. 9. Data from Fig. 7 replotted versus $(\mu^*)^{2/3}$ (eq. (10)).

Note, however, that the two data sets pertaining to the two different gelatin concentrations do not collapse onto a single master curve (here a straight line). That is, the fracture "rate sensitivity" Γ does not depend on one single structural parameter. This remark must be considered in the light of the finding by Joly-Duhamel *et al* [12] (hereafter abbreviated as JHAD) that, for gels of various gelatin concentrations, glycerol contents and thermal histories, there is a one-to-one correspondence between the storage modulus μ and the so-called helix concentration c_{hel}. This latter structural parameter, directly obtained from optical activity measurements, is interpreted as proportional to the length of triple-helix cross-links per unit volume of gel. One might then be tempted to think that the modulus μ contains essentially all the mecano-structural information about the gel. That such is not the case is shown by two observations :

(i) JHAD also show that the loss modulus μ'' does not depend on c_{hel} only, but also on e.g. the gelatin concentation c.

(ii) A non universal behavior was also found by Bot *et al* [6] for the non-linear part of the stress response in compression and in shear - a result confirmed by our own data.

We therefore now turn to the results of series C, which involve gels with the same history and glycerol content ($\phi = 0$) and four different values of c. As can be seen on Figure 10, $\Gamma/(\mu^*)^{2/3}$ definitely increases with μ^*, i.e. with gelatin concentration. It was shown in JHAD that, in the range of moduli explored here ($\mu > 2$ kPa), gel elasticity is well described as that of a freely-hinged network of triple helix rods with average distance $d \sim (k_BT/\mu)^{1/3}$, i.e. scaling as the mesh length scale ξ. This leaves the $\kappa^{-1} \sim \mu^{2/3}$ scaling unaffected. We are thus led to attributing the residual variation of Γ to a concentration dependence of the viscosity appearing in the poroelastic Darcy law. We propose that this should involve, not the bare solvent viscosity, but an effective one

$$\eta_{eff}(c) = \eta_s \, \Theta(c) \tag{11}$$

including possible contributions from dangling ends, loops attached to the network or free chains, invoked in JHAD and in Tanaka's study [9] of the fracture of chemical gels. In view of the discussion (see Section 4.1) of the order of magnitude of Γ, clearly, $\Theta(c)$ should be $\mathcal{O}(1)$.

A tentative power law fit (Figure 10) yields $\eta_{eff}(c) \sim (\mu^*)^{0.75\pm0.03}$ which, combined with the $\mu^*(c)$ variations

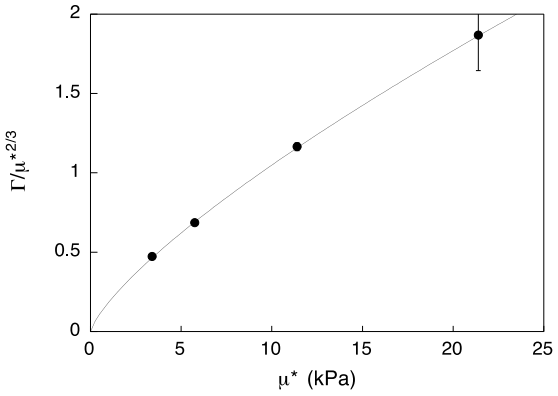

Fig. 10. Data from Fig. 8 replotted as $\Gamma/(\mu^*)^{2/3}$ vs. μ^*. The line is the best power law fit (exponent 0.75).

(see section 3.3), results in $\eta_{eff}(c)/\eta_s \sim c^{1.2}$. The study of creep viscosity in gelatin by Higgs and Ross-Murphy [3] concluded to a $c^{1.1}$ variation. However, their work was concerned with stress levels (σ/μ from 2.10^{-2} to 2.10^{-1}) considerably smaller than those relevant to the active crack tip zone [2]. So, though encouraging, this comparison is of merely indicative value.

Finally, let us come back to the results from series A (same history and gelatin content, various glycerol contents ϕ). A power law fit of the data shown on Figure 5 yields $\Gamma \sim (\mu^*)^{1.2}$. Here again, we must conclude that an increase in ϕ gives rise to an increase, not only of the gel stiffness, but also of the effective viscosity η_{eff}. Following

[2] The viscosities measured in [3] are of order 10^8 Pa sec. This order of magnitude, huge as compared with what we expect here for η_{eff}, must clearly be assigned to the stress range which they investigate. Indeed, far below the yield stress level ($\sigma \ll \sigma^*$), thermally activated CL creep is necessarily extremely slow.

JHAD, an increased stiffness means an increase of c_{hel}, which signals a change of solvent quality. In the unstressed gel, this most probably influences the CL average length as well as the helix fraction. Since changing the Flory interaction parameter shifts helix-coil transitions, it is likely to also affect the structural changes shown by Courty *et al* [32] to result in large variations of optical activity in the large strain regime. We expect the value of η_{eff} to be sensitive to these structural modifications.

In conclusion, we contend here that fracture of chemical and physical gels is controlled by different mechanisms :

– stretched chain scission (chemical gels).

– viscoplastic cross-link yield leading to chain pull-out (physical gels).

Of course, the model formulated here should be tested more completely by studying crack tip dynamics in other physical hydrogels involving CL with different structures, such as ionically cross-linked alginates. More work will also be needed along two directions : (a) characterization of creep dynamics at larger stress levels than those used in reference [3], and of its dependence on solvent viscosity; (b) more detailed study of slow crack motion, aimed at improving the reliability of $\mathcal{G}_0$-determinations as well as at testing possible effects of bulk poroelasticity.

We are gratelul to C.Y. Hui for an enlightening discussion. We thank L. Legrand for his contribution to the analysis of the gel light-scattering properties.

References

1. A.H. Clark, S.B. Ross-Murphy, Adv. Polymer Sci. **83**, 57 (1987).
2. K. te Nijenhuis, Adv. Polymer Sci. **130**, 1 (1997).
3. P. G. Higgs, S. B. Ross-Murphy, Int. J. Biol. Macromol. **12**, 233 (1990).
4. T. van Vliet, P. Walstra, Faraday Discuss. **101**, 359 (1995).
5. K. Y. Lee, D. J. Mooney, Chem. Rev., **101**, 1869 (2001).
6. A. Bot, I.A. van Amerongen, R.D. Groot, N.L. Hoekstra, W.G.M. Agterof, Polymer Gels and Networks **4**, 189 (1996).
7. H. Mc Evoy, S. B. Ross-Murphy, A. H. Clark, Polymer **26**, 1483 (1985).
8. D. Bonn, H. Kellay, M. Prochnow, K. Ben-Djemiaa, J. Meunier, Science **280**, 265 (1998).
9. Y. Tanaka, K. Fukuao, Y. Miyamoto, Eur. J. Phys. E **3**, 395 (2000).
10. H. J. Kong, E. Wong, D. J. Mooney, Macromolecules **36**, 4582 (2003).
11. T. Baumberger, C. Caroli, D. Martina, Nature Materials, doi:10.1038/nmat1666 (2006).
12. C. Joly-Duhamel, D. Hellio, A. Ajdari, M. Djabourov, Langmuir **18**, 7158 (2002).
13. J.-L. Laurent, P. A. Janmey, J. D. Ferry, J. Rheol. **24**, 87 (1980).
14. D.L. Johnson, J. Chem. Phys. **77**, 1531 (1982).
15. T. Tanaka, L.O. Hocker, G. B. Benedek, J. Chem. Phys. **59**, 5151 (1973).
16. T. Baumberger, C. Caroli, O. Ronsin, Eur. Phys. J. E**11**, 85 (2003).

17. R. S. Rivlin, A. G. Thomas, J. Polymer Sci. **10**, 291 (1953).
18. J.W. Rudnicki, T-C Hsu, J. Geophys. Res. B **93**, 3275 (1988).
19. A. Ruina, M. Sc. Thesis, Brown University, 1978. (Can be downloaded from http://ruina.tam.cornell.edu).
20. G. J. Lake, A.G. Thomas, Proc. R. Soc. London A **300**, 108 (1967).
21. H.K. Mueller, W.G. Knauss, Trans. Soc. Rheol. **15**, 217 (1971).
22. A.N. Gent, J. Schultz, J. Adhesion **3**, 281 (1972).
23. A. N. Gent, Langmuir **12**, 4492 (1996).
24. P.G. de Gennes, C. R. Acad. Sci. Paris, II **307**, 1949 (1988).
25. C.-Y. Hui, D. B. Xu, E.J. Kramer, J. Appl. Phys. **72** 3294 (1992).
26. , E.A. Brenner, Phys. Rev. E **71** 036123 (2005).
27. P. G. Higgs, R. C. Ball, Macromolecules **22**, 2432 (1989).
28. K. Nishinari, S. Koide, K. Ogino, J. Physique **46**, 793 (1985).
29. B.N.J. Persson, J. Chem. Phys. **110**, 9713 (1999).
30. C.-Y.Hui, A. Jagota, S. J. Bennison, J. D. Londono, Proc. R. Soc. London A **459**, 1489 (2003).
31. B. R. Lawn, Fracture of brittle solids — 2nd edn, Cambridge, University Press (1993).
32. S. Courty, J.L. Gornall, E.M. Terentjev, Biophys. J. **90**, 1019 (2006).
33. E. Raphaël, P.G. de Gennes, J. Phys. Chem. **96**, 4002 (1992).
34. L.O. Fager, J.L. Bassani, C.-Y. Hui, D.B. Xu, Int. J. Fract. **52**, 119 (1991).

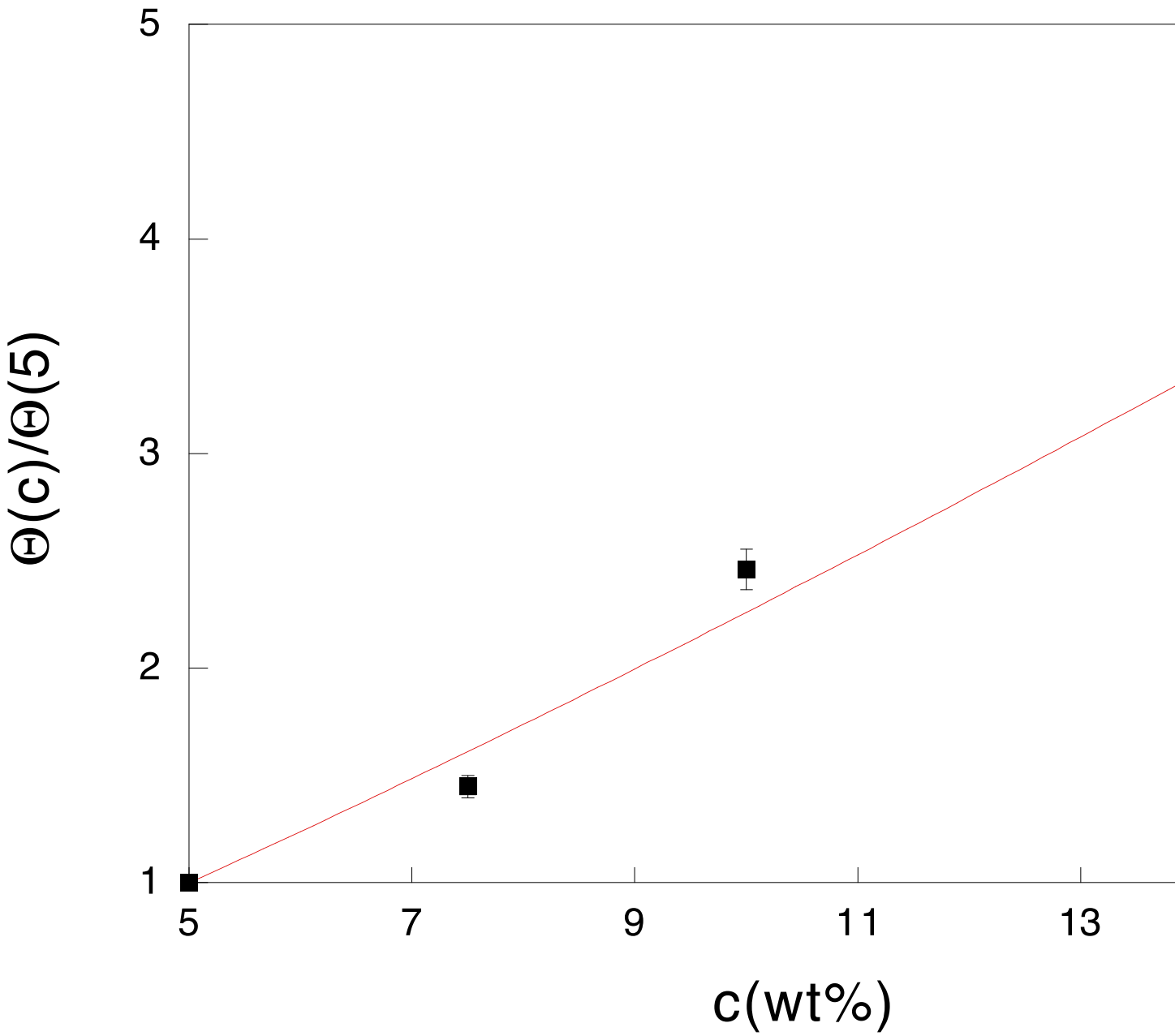
5
4
3
2
1
Θ(c)/Θ(5)
5
7
9
11
13
c(wt%)